



Research article

A long short-term memory relation network for real-time prediction of patient-specific ventilator parameters

Xihe Qiu¹, Xiaoyu Tan², Chenghao Wang¹, Shaotao Chen¹, Bin Du³ and Jingjing Huang^{4,5,*}

¹ School of Electronic and Electrical Engineering, Shanghai University of Engineering Science, Shanghai 201620, China

² INF Technology (Shanghai) Company Limited, Shanghai 201203, China

³ Yanshan Electronics of Beijing, Beijing 100192, China

⁴ ENT institute and Department of Otorhinolaryngology, Fudan University, Shanghai 200031, China

⁵ Shanghai Municipal Key Clinical Specialty, Shanghai 200031, China

* **Correspondence:** Email: gennie_xuan@163.com.

Abstract: Accurate prediction of patient-specific ventilator parameters is crucial for optimizing patient-ventilator interaction. Current approaches encounter difficulties in concurrently observing long-term, time-series dependencies and capturing complex, significant features that influence the ventilator treatment process, thereby hindering the achievement of accurate prediction of ventilator parameters. To address these challenges, we propose a novel approach called the long short-term memory relation network (LSTMRnet). Our approach uses a long, short-term memory bank to store rich information and an important feature selection step to extract relevant features related to respiratory parameters. This information is obtained from the prior knowledge of the follow up model. We also concatenate the embeddings of both information types to maintain the joint learning of spatio-temporal features. Our LSTMRnet effectively preserves both time-series and complex spatial-critical feature information, enabling an accurate prediction of ventilator parameters. We extensively validate our approach using the publicly available medical information mart for intensive care (MIMIC-III) dataset and achieve superior results, which can be potentially utilized for ventilator treatment (i.e., sleep apnea-hypopnea syndrome ventilator treatment and intensive care units ventilator treatment).

Keywords: neural networks; ventilator parameter prediction; machine learning; important feature selection; long short-term memory

1. Introduction

Ventilators are essential medical devices utilized in intensive care units (ICUs) to prevent respiratory failure during routine treatment, emergency care, or surgery. They play a significant role in treating severe and life-threatening infections, including coronavirus disease 2019 (COVID-19) [1]. During ventilator operation, clinicians must adjust the parameters in response to the patient's real-time physical state, test results, and symptom analysis. However, the setting of these parameters [2] heavily relies on clinicians' expertise, and improper use can lead to serious complications [3], such as respiratory alkalosis and hypoxemia, which can lead to serious complications (i.e., respiratory failure affecting kidney function), raising the risk of patient death [4, 5].

Automatic prediction methods based on the principles of automatic control and machine learning (ML) have been proposed to aid in setting optimal ventilator parameters and reduce medical errors. Traditional automatic control methods [6–11] provide solutions for automatically predicting optimal ventilator settings. Nevertheless, they are limited to analyzing characteristic data, and in the complex medical environment of the ICU, these control systems still rely heavily on the medical experts' experience. Automation-based systems suffer from low accuracy and efficiency when dealing with high-dimensional, data-intensive clinical scenarios.

ML algorithms have become increasingly popular in various fields [12, 13] such as machine vision, intelligent driving, and games. In medicine and healthcare, ML algorithms are extensively used for clinical decision support [14, 15], exhibiting a superior performance in handling high-dimensional and massive data [16, 17]. As a result, they have become a powerful tool for assisting in handling large amounts of high-dimensional data [18]. The use of ML algorithms can help eliminate subjective factors in the diagnosis process, providing accurate predictions and decision-making recommendations for physicians [19, 20]. Therefore, ML algorithms offer potential options for automatic ventilator parameter control.

A dozen of ML models [21–25] have been proposed for predicting ventilator parameters. These approaches range from a support vector regression [21], a k -nearest neighbor algorithm, an artificial neural network (ANN) [22], and a decision tree Bootstrap aggregation [23], to more recent reinforcement learning (RL) based methods [24]. The aforementioned ML methods have achieved a superior performance; however, they exhibit two essential limitations. First, they only focus on the correlation between ventilator parameters and patient vital signs, thereby neglecting the fact that predicting ventilator parameters involves optimizing time-series prediction, and does not consider the time-series long-term effects will compromise the accuracy of the models. Second, prior studies have not addressed the simultaneous prediction of both continuous parameters (i.e., positive end-expiratory pressure (PEEP), fraction of inspired oxygen (FiO_2) and tidal volume (TV), and discrete parameters (i.e., ventilator modes) in ventilator parameter prediction. Therefore, it is important to explore methods for more accurate and efficient prediction of optimal ventilator parameters by incorporating both spatial and time-series features and accounting for both continuous and discrete parameters.

To achieve a precise prediction of optimal ventilator parameters that meets the clinical design requirements, we propose a novel approach called the long short-term memory relation network (LSTMRnet). Our approach incorporates a feature selection process, which enhances the influence of critical information on prediction results by identifying important features that significantly impact the ventilator parameter selection. Additionally, the time-series information collection process is

designed to capture time-series information and to improve the overall prediction capabilities of the model. To facilitate a more effective feature selection, we develop a unique selection process that utilizes XGBoost [26] to generate predictions, followed by the SHapley Additive exPlanations (SHAP) algorithm [27] for an interpretability analysis of relevant features. Through this process, we are able to determine the importance ranking of features in the ventilator treatment process and select the significant features that influence ventilator parameters. We employ multiple layered long short-term memory neural networks (LSTM) [28] to capture the time-series information of features. Then, we combine the embeddings of both spatial and time-series information from the two processes to enhance the prediction performance of our model.

The main contributions of this study are as follows.

- In this work, we propose LSTMRnet as a novel approach for predicting ventilator parameters accurately from time-series data. Our approach surpasses the performance of previous ML and time-series models by effectively capturing complex features selected by an important feature selector, enabling long-range temporal dependence observation, and improving prediction accuracy. Additionally, our method can predict both continuous and discrete parameters.
- To obtain a more comprehensive and rich feature representation of both crucial spatial features and time-series features, we design a feature selection process, and the embeddings produced by the feature selector are concatenated with LSTM-generated time-series feature embeddings for a more accurate prediction.
- Extensive validations are performed on the public benchmark dataset (i.e., MIMIC-III). Our method achieves a significant performance, exceeding the state-of-the-art methods by a wide margin.

The rest of this paper is organized as follows. The detail of data processing and a detailed description of our proposed model is shown in Section 3. Experimental details and main results are presented in Section 4. Section 5 provides a comparison of experiments. Finally, we conclude the paper in Section 6.

2. Related works

Automatic prediction methods for optimal ventilator parameters have been proposed to aid in the setting of optimal ventilator parameters and to reduce medical errors. These methods are primarily based on the principles of traditional automatic control and ML.

2.1. Traditional automatic prediction methods

Nemoto et al. [6] combined automatic control theory and proposed a mathematical model for optimal ventilator settings. The ventilator is controlled by a fuzzy logic algorithm that measures the patient's vital signs such as heart rate, TV, respiratory rate, and arterial oxygen saturation. Rees et al. [7] described the preferred settings and adverse effects of ventilator therapy using penalty functions and mathematical models for oxygen delivery, carbon dioxide delivery, and lung mechanics. Karbing et al. [8, 29] proposed a closed-loop system that used a proportional-integral-derivative (PID) algorithm to automatically control the ventilator by adjusting oxygen flow, respiratory rate, and TV based on continuous feedback from patient vital signs. Chatburn et al. [9] combined a closed-loop system with a target scheme by controlling the ventilator

towards six basic target schemes: setpoint, servo-target, adaptive target, optimal target, and intelligent target. Marco et al. [10] used flow and pressure waveform analyses generated by the ventilator to optimize the flow rate of chronic obstructive pulmonary. Karbing et al. [11] presented an open-loop system that analyzes pulse oximetry and breathing tubes to provide a solution for optimal ventilator settings. Conclusively, traditional automatic control methods have been designed to analyze some characteristic data. However, in the complex medical environment of the ICU, the above control systems still heavily rely on the experience of medical staff, and the above automation-based systems still suffer from low accuracy and efficiency when dealing with high-dimensional, data-intensive clinical scenarios.

2.2. ML based automatic prediction methods

Previous studies have proposed various ML models such as decision trees, XGBoost, and support vector regression for predicting ventilator parameters [21, 30]. Additionally, the k -nearest neighbor algorithm, logistic regression, and decision trees have been used for an early prediction of respiratory parameters [31, 32]. Akbulut et al. [22] proposed an artificial neural network (ANN) model that predicts the output of frequency, TV and FiO_2 , and employs Softmax activation to predict whether the output is pressure-supported or volume-supported. Ghazal et al. [23] combine a complex decision tree with Bootstrap aggregation for predicting ventilator parameters. Venkata et al. [33] present a respiratory parameter recommendation system based on an ANN and particle swarm optimizer to predict the ventilator parameter settings for patients under pressure support ventilation (PSV) mode. Radhakrishnan et al. [25] proposed a respiratory parameter recommendation system based on multilayer perceptron (MLP) to predict changes in the delivered FiO_2 , ventilator mode, and PEEP of mechanical ventilators. However, the above-mentioned methods either did not consider important information that affects ventilator parameters or overlooked the time-series information in ventilator parameter prediction. Peine et al. [24] proposed the Q-learning algorithm proposed to optimize the settings of continuous parameters in ventilators, such as PEEP, the FiO_2 , and TV. Ventilator parameters include both continuous parameters (such as PEEP, FiO_2 , and TV) and discrete parameters (such as ventilator modes). However, previous studies have not considered the simultaneous prediction of both continuous and discrete parameters.

3. Methods

The proposed model consists of two key processes: feature selection and time-series information capture.

The ventilator parameters include continuous parameters (FiO_2 , PEEP, TV, O_2 flow, Rate) and discrete parameters (ventilator mode). FiO_2 represents the concentration of oxygen in the inhaled gas, which controls the output oxygen of the ventilator. PEEP is a device that maintains a certain positive pressure in the respiratory tract during the end of exhalation, avoiding early alveolar closure and achieving the goal of increasing blood oxygen. TV refers to the amount of air either inhaled or exhaled during calm breathing; it is related to age, gender, surface volume, respiratory habits, and body metabolism. O_2 flow is the rate at which the ventilator delivers TV, adjusted according to the patient's needs. The rate refers to the number of breaths per minute the ventilator delivers to the patient. There are mainly 32 different ventilator modes for discrete parameters, and the ventilator

mode sets different ventilator treatment plans based on the patient's physical condition.

The overall framework of our proposed LSTMRnet approach is depicted in Figure 1. The prediction is divided into two sections: a classification task for the prediction of discrete respiratory data and a regression task for the prediction of continuous breathing parameters. Initially, features are predicted using XGBoost and interpreted using the SHAP interpretation model. Then, the selected features are passed through a multi-layer perceptron (MLP). Concurrently, LSTM networks are utilized to capture time-series information from all patient vital signs, which is subsequently fed into an MLP. Finally, we concatenate the information obtained from these two processes to achieve a ventilator parameter prediction.

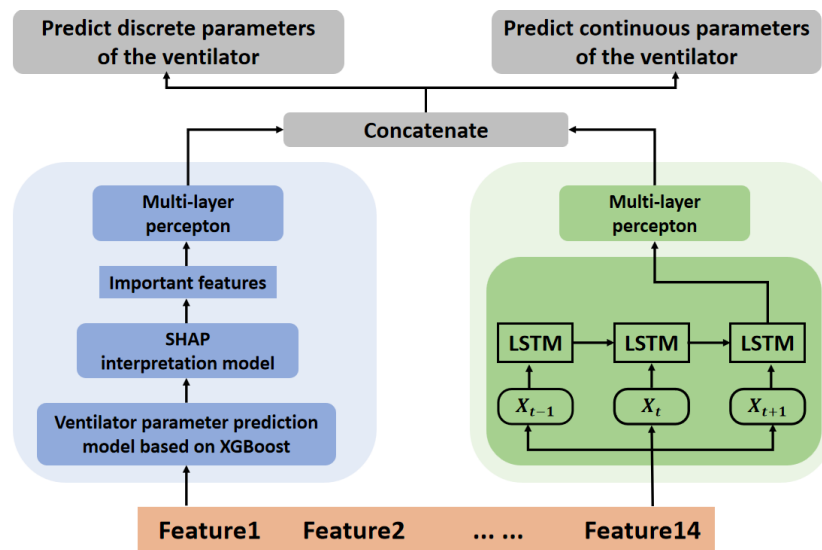


Figure 1. The overall framework of LSTMRnet.

We introduce the LSTMRnet approach for predicting respiratory parameters. The model takes 14 patient signs as the input and generates predictions for both continuous and discrete respiratory parameters as output. The training procedure is presented in Algorithm 1.

Algorithm 1 The training process of LSTMRnet

Input: features x

Output: ventilator parameter

- 1: performs XGBoost classification through Equation (3.1) and optimize the model by Equation (3.5).
 - 2: performs feature selection using the SHAP framework through Equations (3.6) and (3.7).
 - 3: input the time-series feature into the LSTM model and get h_t .
 - 4: concatenate h_t with x_z and output the final prediction results with Equation (3.8).
 - 5: optimize the model with
 - 6: **return** discrete and continuous parameters of the ventilator
-

3.1. Important feature selection process

As shown in Figure 2, we design a unique process to obtain the important features. This process incorporates the XGBoost algorithm and the SHAP interpretable model for selecting significant features. Among the vital ventilator parameters, the mode of ventilation holds a particular importance. To classify the ventilator mode, we construct a ventilator parameter prediction model using the XGBoost algorithm, with the patient's vital signs as the input. Subsequently, an interpretability analysis is conducted using the SHAP interpretation model to identify the influential features that impact the ventilator treatment process.

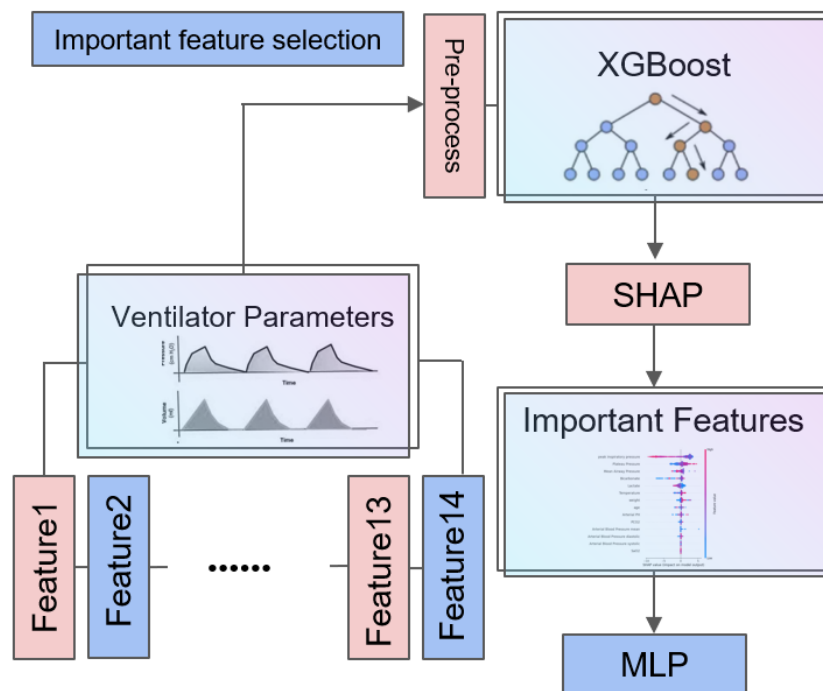


Figure 2. An overview of the important feature selection process.

XGBoost [34] is an improved algorithm derived from gradient-boosted decision trees. Unlike GBDT, which only utilizes a first-order Taylor expansion for the error component; XGBoost employs a second-order Taylor expansion to approximate the learning target. This enables the utilization of both first-order and second-order derivatives. By integrating multiple decision trees, XGBoost improves the prediction accuracy. It achieves this by continuously splitting features to construct new decision trees and adding new functions to fit the residuals between the predicted and actual values from the previous round. The model's prediction value, denoted as \hat{y} , is defined as follows:

$$\hat{y} = \sum_{k=1}^K g_k(x_i), g_k \in G, \quad (3.1)$$

where K is the number of decision trees, G is the function space consisting of K decision trees, and

$g_k(x_i)$ is the function of the i decision tree

To simplify the model and prevent model overfitting, a regular term is added to the objective function to learn the set of G functions of K decision trees. Assuming φ is the function sets of K decision trees, H is the number of leaf nodes, ω is the leaf node weight matrix, and α and β are the corresponding parameters of the regular term, the objective function is defined as:

$$\mathcal{L}(\varphi) = \sum_i (y_i - \hat{y}_i)^2 + \sum_k \left(\alpha H + \frac{1}{2} \beta \|\omega\|^2 \right). \quad (3.2)$$

To increase prediction accuracy, the XGBoost algorithm constructs the loss function using a second-order Taylor expansion, which has a faster convergence rate compared with the first-order Taylor expansion. The Boosting algorithm is an additive model (i.e., at each iteration, a new decision tree is added to the original one, and the residuals of the previous prediction are fitted by learning a new function $g(x)$). Thus, the objective function is transformed into the following

$$\mathcal{L}^t = \sum_{i=1}^n \left[y_i - (\hat{y}_i^{t-1} + g_t(x_i)) \right]^2 + \alpha H + \frac{1}{2} \beta \|\omega\|^2. \quad (3.3)$$

After second-order Taylor expansion:

$$\tilde{\mathcal{L}}^t = \sum_{i=1}^n \left(n_i g_t(x_i) + \frac{1}{2} m_i g_t^2(x_i) \right) + \alpha H + \frac{1}{2} \beta \sum_{j=1}^T \omega_j^2, \quad (3.4)$$

where n_i is the first-order partial derivative and m_i is the second-order partial derivative. According to the objective function and the convex optimization method, the optimal objective function of the decision tree model is obtained as follows:

$$\text{Obj}(t) = -\frac{1}{2} \sum_{j=1}^T \frac{(\sum_{i \in I} n_i)^2}{\sum_{i \in I} m_i + \beta} + \alpha H. \quad (3.5)$$

The decision tree models' performance is evaluated using the optimal objective function. The lower the output of this function, the better the decision tree model's performance. The hyperparameters of this model include the learning rate, the minimum number of leaves, the maximum depth of the tree, the number of trees, the regularization factor, and some features.

ML algorithms have demonstrated exceptional predictive capabilities. However, their intricate structures often make it challenging to provide explanations based on the original mathematical model. In our experiments, we employ the XGBoost model for classifying ventilator modes. Although the XGBoost model itself has a complex structure and limited interpretability, we address this limitation by introducing the SHAP interpretable model to enhance its interpretability.

Derived from coalitional game theory, SHAP is an interpretable model that explains black box ML models [35]. It utilizes the Shapley value as a uniform indicator to quantify the contribution of each input feature to the prediction result. By calculating the Shapley value for each feature, the model determines their individual contributions and summarizes them to obtain the final interpretation result. Based on these interpretation results, the important features influencing the selection of ventilator parameters are identified.

The output of the XGBoost prediction model is the pattern prediction result of the ventilator. By calculating the Shapley value for each input feature, we can determine the contribution of each feature. Assuming that m is the original model explained, F is the number of input features, σ^{SHAP} is the Shapley value of the feature, and z is a Boolean type representing whether the feature is a missing value; the SHAP explanatory model is described as:

$$m(z) = \sigma_0^{\text{SHAP}} + \sum_{i=1}^F \sigma_i^{\text{SHAP}} z_i. \quad (3.6)$$

The Shapley value of each feature represents the feature's contribution to the overall result. The larger the Shapley value, the greater the impact of the feature on the prediction result. When $z = 0$, it means that the missing value does not contribute to the importance of the feature. We utilize the SHAP explanatory model to extract important features and improve the reliability of the prediction results [36, 37]. The important feature x_z can be achieved by:

$$x_z = m(x). \quad (3.7)$$

Moreover, the SHAP model is applied to interpret the ventilator pattern prediction model, aiding in the identification of critical factors that influence ventilator treatment, hence providing clinicians with better clinical decision support.

3.2. Time-series information capture process

In clinical scenarios, the patient's vital signs exhibit time-series characteristics, where the next stage of the patient's state depends on both recent and distant past states and events. Time-series data of a patient's vital signs plays a critical role in forecasting ventilator parameters, with long-term predictions being more meaningful for decision support than short-term predictions.

To capture the time-series data of features, we employ the LSTM model [38]. As a recurrent neural network (RNN) model, LSTM is well-suited for modeling clinical data in time series prediction tasks. By incorporating forgetting units, input units, and output units to model long and short-term dependencies, LSTM effectively addresses the challenge of long-term dependence in RNNs. The LSTM model captures the time-series information, which is subsequently output by the MLP network to generate accurate predictions.

The elements of the LSTM model include the candidate cell state: $\tilde{c}_t = \tanh(W_{xc}x_t + W_{hc}h_{t-1} + b_c)$, input gate: $i_t = \sigma(W_{xi}x_t + W_{hi}h_{t-1} + b_i)$, forget gate: $f_t = \sigma(W_{xf}x_t + W_{hf}h_{t-1} + b_f)$, output gate: $o_t = \sigma(W_{xo}x_t + W_{ho}h_{t-1} + b_o)$, updated cell state: $c_t = f_t c_{t-1} + i_t \tilde{c}_t$, and hidden state: $h_t = o_t \tanh(c_t)$, where σ represents the sigmoid function, \tanh represents the hyperbolic tangent function, weights, and biases are denoted by W and b on different states, respectively.

Here, we concatenate the selected important static feature x_z with the last hidden state h_t and then pass the concatenated information to another MLP model o , followed by a Softmax layer:

$$h_{\text{cat}} = o(x_z || h_t), \hat{y}_t^{\text{cls}} = \text{softmax}(W_{\text{cls}} h_{\text{cat}} + b_y), \hat{y}_t^{\text{reg}} = W_{\text{reg}} h_{\text{cat}} \quad (3.8)$$

where the last linear layer of weights and biases are denoted by W and b , respectively, and $||$ indicates

the concatenation. The LSTM can be optimized by the following cross-entropy loss:

$$\mathcal{L}_{CE}(y, \hat{y}) = -\frac{1}{N} \sum_{i=1}^N \sum_{j=1}^C y_{ij} \log(\hat{y}_{ij}), \quad (3.9)$$

with total class number of C , and mean-squared-error regression loss:

$$\mathcal{L}_{MSE}(y, \hat{y}) = \frac{1}{N} \sum_{i=1}^N (y_i - \hat{y}_i)^2. \quad (3.10)$$

Finally, the time-series information collection process is combined with the significant feature selection process to improve the prediction performance. For the prediction of ventilator parameters, where both continuous and discrete parameters are involved, we treat the prediction of discrete parameters as a classification task and the prediction of continuous parameters as a regression task. To effectively address these tasks, the two processes utilize distinct activation functions as outputs, specifically tailored for classification and regression in respiratory parameter prediction, respectively.

3.3. Data description and experiment setup

The information comes from the Medical Information Mart for Intensive Care III (MIMIC-III). The MIMIC III database is comprised of information about patients in large tertiary care hospitals, including vital signs, medications, laboratory measurements, medical orders, procedure codes, diagnosis codes, impact reports, length of stay, survival data, and a variety of other information. As illustrated in Figure 3, this database contains 58,976 ICU admissions from 2001 to 2012, with a total of 46,520 patients, 5,854 of whom unfortunately died during their hospitalization, and a mortality rate of 9.9% in all ICU units.

We extract the ventilator-related data from the MIMIC III dataset to establish the following datasets: chartevent (containing the patient's vital signs), lab event (containing the patient's laboratory lab records), d items, and d lab items, where d items and d lab items are utilized to search for the ITEMID with the corresponding feature.

We extract the data in chartevent and lab events according to the ITEMID corresponding to the feature and save the SUBJECT ID, ITEMID, CHARTTIME (time from ITEMID), and VALUE columns of the extracted data to a separate dataset. To completely comprehend the influence of the ventilator parameter settings on patients, we retrieve a dataset with 20 attributes, including patient-specific lab test results and monitoring measurements. These attributes are composed of fractional oxygen concentration in inspiratory air (FiO_2), PEEP, respiratory rate, tidal volume (TV), O_2 flow, ventilator mode, inspiratory plateau pressure, mean airway pressure, partial pressure of carbon dioxide (PCO_2), peak inspiratory pressure, mean arterial blood pressure mean, arterial blood oxygen saturation (SaO_2), arterial diastolic pressure, arterial blood pressure diastolic, arterial blood pressure systolic, arterial pH, lactate, temperature, bicarbonate, weight, and age.

In total, there are 32 ventilator modes. Those 32 ventilator modes are labeled by the encoder with integers from 0 to 31. After processing these 14 datasets, a dataset containing 12,519 individuals with time series is obtained. The 14 datasets are merged with the SUBJECT ID (which is the primary key linking all datasets) and the missing values are initially filled using the values within the proximity of 24 hours. To ensure data integrity, the average of each feature value is utilized to fill in the missing

data. Additionally, the combined dataset contains a substantial number of abnormal values, such as values of unusual size and null values. As individual abnormal data may be generated due to recording errors and have no reference relevance, we delete all null and abnormal values in this study to improve the quality of the dataset. The data set is randomly divided into a training set of 80% and a validation set of 20%.

The experiments are performed using Python 3.9 and Scikit-learn 0.24.2. The operating system employed is Windows 10 64-bit. The CPU is an AMD Ryzen7 3700X 8-Core Processor @3.59GHZ with 16GB of RAM and an NVIDIA GeForce RTX 2070 SUPER graphics card.

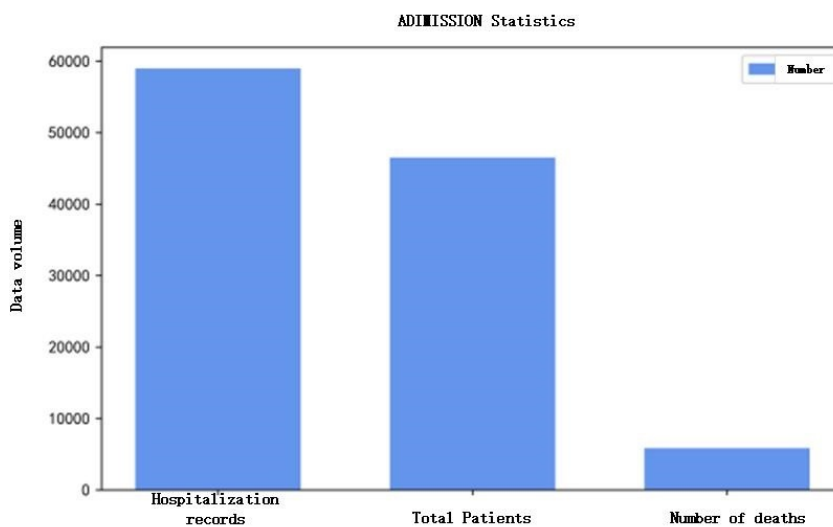


Figure 3. Statistical chart of patient information.

3.4. Hyper-parameters settings and model evaluation

During the important feature selection process, key hyperparameters include *leaning_rate*, *n_estimators*, *max_depth*, *reg_lambda*, *gamma*, *reg_alpha*, *subsample*, and *min_child_weight*. The XGBoost model is utilized to classify respiratory patterns using the obtained optimal model and parameters. The optimal parameters of the XGBoost model are presented in Table 1.

Table 1. Optimal parameters of XGBoost model.

Parameter name	Parameter meaning	Optimal parameters
<i>leaning_rate</i>	Learning Rate	0.3
<i>n_estimators</i>	Number of weak learners	500
<i>max_depth</i>	Maximum depth of tree	5
<i>reg_lambda</i>	L2 regularisation term	2
<i>gamma</i>	Minimum loss rate for node splitting	0.1
<i>reg_alpha</i>	L1 regularisation term	0.1
<i>subsample</i>	Proportion of random sampling	1
<i>min_child_weight</i>	Minimum leaf node sample weights	1

In the time-series information capture process of the LSTM model, crucial hyperparameters such as `learning_rate`, `n_estimators`, `reg_lambda`, `reg_alpha`, `subsample`, `batch_size`, and LSTM units are considered. The optimal parameter values for the LSTM model are shown in Table 2.

Table 2. Optimal parameters of LSTM model.

Parameter name	Parameter meaning	Optimal parameters
<code>learning_rate</code>	Learning Rate	0.1
<code>n_estimators</code>	Number of weak learners	500
<code>reg_lambda</code>	L2 regularisation term	2
<code>reg_alpha</code>	L1 regularisation term	0.1
<code>subsample</code>	Proportion of random sampling	1
<code>Batch_size</code>	Batch size	50
LSTM units	Number of LSTM cells	50

Regression task assessment measures include mean squared error (MSE), mean absolute error (MAE), and R^2 Score, whereas classification task evaluation metrics include Precision, F1, and Recall. To better evaluate the performance of the prediction model with both regression and classification tasks, we use six evaluation metrics: MAE, MSE, R^2 Score, Precision, F1, and Recall. These six metrics are defined as follows.

$$\text{MAE} = \frac{1}{n} \sum_{i=1}^n |y_i - \hat{y}_i| \quad (3.11)$$

$$\text{MSE} = \frac{1}{n} \sum_{i=1}^n (y_i - \hat{y}_i)^2 \quad (3.12)$$

$$\text{R}^2_{\text{Score}} = 1 - \frac{\sum_i (y_i - \hat{y}_i)^2}{\sum_i (\bar{y} - \hat{y}_i)^2} \quad (3.13)$$

where: y_i denotes the true value, \hat{y}_i denotes the predicted value, and \bar{y} denotes the mean value.

$$\text{Precision} = \frac{TP}{TP + FP} \quad (3.14)$$

$$\text{Recall} = \frac{TP}{TP + FN} \quad (3.15)$$

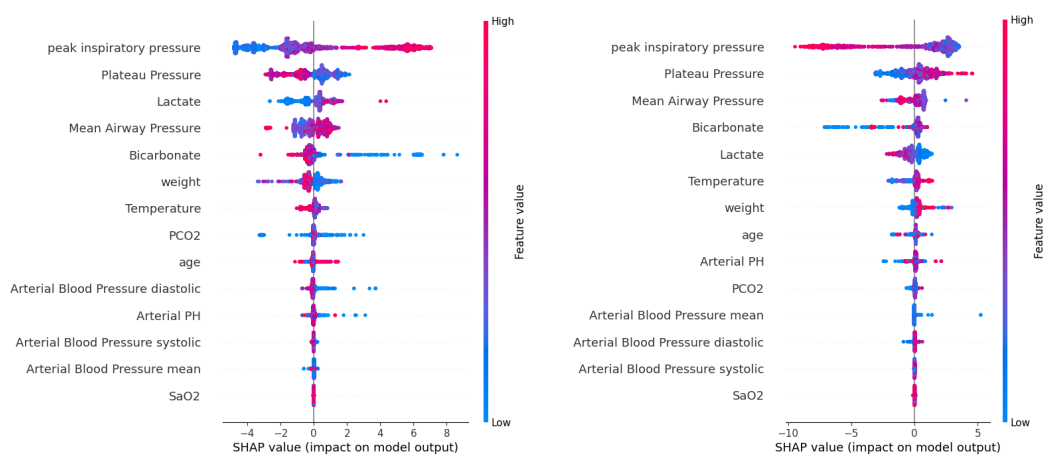
$$\text{F1_Score} = \frac{2 \times \text{Precision} \times \text{Recall}}{\text{Precision} + \text{Recall}} \quad (3.16)$$

4. Main results

In this section, we analyze the performance of our model on the MIMIC-III, evaluate its performance against a number of baselines, and examine the results of the experiments.

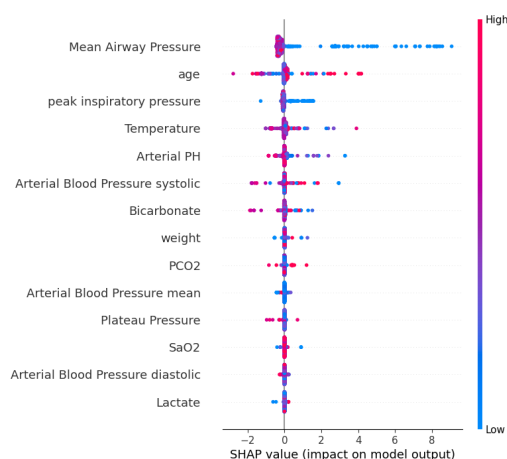
4.1. Important parameter analysis

In this paper, we use the SHAP model to perform an interpretive analysis of the XGBoost model's output. The interpretive results are shown in Figure 4. Figure 4(a) shows the analysis of the ventilator mode CMV/ASSIST/AutoFlow's effect according to the characteristics, Figure 4(b) shows the analysis of the effect of ventilator mode CPAP/PSV/, and Figure 4(c) depicts the analysis of ventilator mode Standby. As shown in Figure 4, the Peak inspiratory pressure (peak airway pressure), Plateau Pressure (inspiratory plateau pressure), Lactate (lactate), Mean Airway Pressure (mean Lactate, Mean Airway Pressure, and Bicarbonate have a greater influence on the model for both CMV/ASSIST/AutoFlow and CPAP/ASV ventilator modes. The influence of Mean Airway Pressure and age are prominent in the Standby model. According to the SHAP value, peak inspiratory pressure has the greatest effect on ventilator parameters and exhibits a complex nonlinear relationship.



(a) CMV/ASSIST/AutoFlow Feature analysis

(b) CPAP/PSV Feature analysis



(c) Standby Feature analysis

Figure 4. Feature analysis chart.

Figure 5 shows the feature dependence plots of Peak inspiratory pressure (SHAP), SaO₂ (oxygen saturation), Weight (body weight), and Plateau Pressure (PH). Figure 5(a) shows the change of peak

inspiratory pressure on blood PH. The experimental results show the effect of increasing blood PH from -1.5 to 1 on the SHAP value of peak inspiratory pressure, with red dots indicating a high PH value and blue dots demonstrating a low PH value.

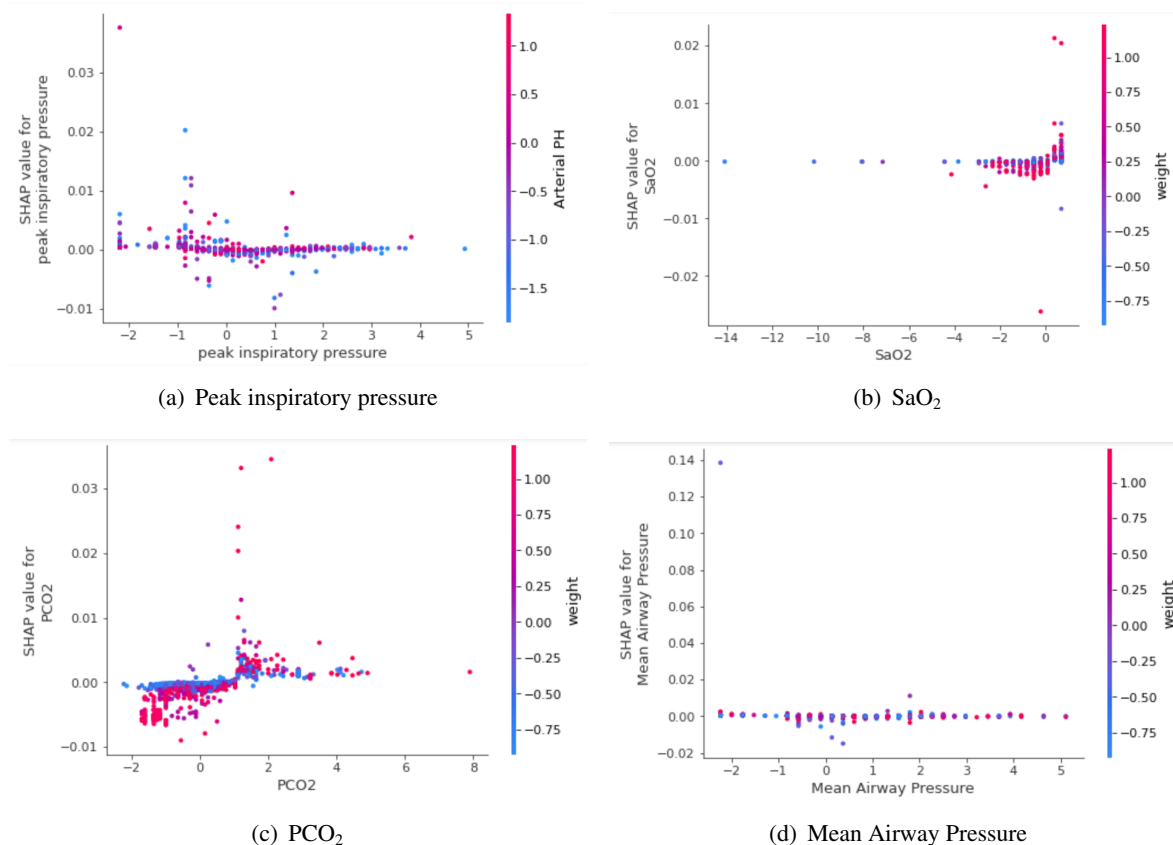


Figure 5. Feature dependence analysis chart.

When the peak inspiratory pressure is low, the blood PH is predominantly red, indicating that the blood PH is greater during this time. As the patient's peak inspiratory pressure increases, the value of SHAP is nearly stable and the blood PH value gradually changes from red to blue, which indicates that the interaction coefficient between peak inspiratory pressure and blood PH should be negative. Figure 5 (a),(b),(c) show the interrelationship between SaO₂ (arterial oxygen saturation), PCO₂, mean airway pressure (mean airway pressure) to Weight (body weight), respectively. These three figures indicate the following: SHAP values remain stable as SaO₂ (arterial oxygen saturation) increases; the Weight value increases as the patient's arterial oxygen saturation rises, indicating a possible positive correlation between arterial oxygen saturation and patient weight. When the Weight value is relatively large and the PCO₂ value is less than 1.5, the value of SHAP is mostly negative and negatively correlated with the Weight value. After the PCO₂ value becomes greater than 1.5, the change of the SHAP value increases with the Weight value and is positive, which indicates that the patient's weight will affect the value of PCO₂ during ventilator treatment. SHAP values are essentially stable at different mean airway pressures, regardless of the patient's weight, indicating that mean airway pressure exerts minimal influence on the patient.

The importance of ranking of the features of the SHAP model is shown in Figure 6, where the

most important feature in the ventilator mode selection process is the peak inspiratory pressure [39]. The ventilator therapy is determined by the ventilator mode [40,41]. To improve treatment efficacy, it is beneficial to provide the proper ventilator mode for patients with varied degrees of respiratory illness. In addition to peak inspiratory pressure, vital signs such as mean airway pressure, inspiratory plateau pressure, bicarbonate, and lactate are also important factors that influence ventilator therapy [42]. In clinical application scenarios, the clinicians can adjust the ventilator mode according to the characteristics of the patient's mean airway pressure, inspiratory plateau pressure, bicarbonate, and lactate.

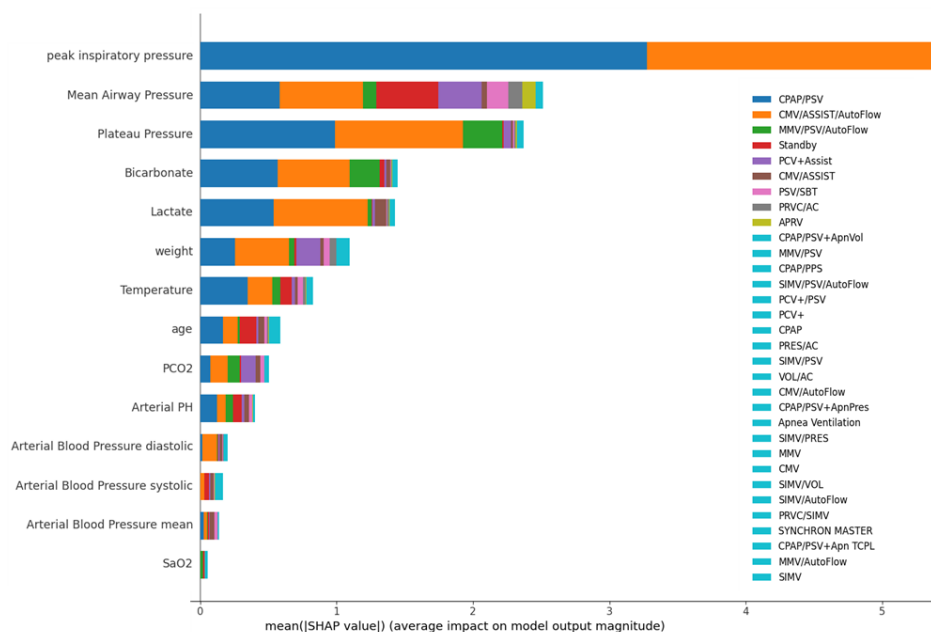


Figure 6. Feature importance ranking.

4.2. Comparative experimental results of different models

We compare our model with the following baseline ML algorithms: MLP, LSTM, LSTM+Logistic, and LSTM+MLP.

MLP: input all features directly into the MLP model to predict ventilator parameters, without any feature selection process.

LSTM: input all features directly into the LSTM model to predict ventilator parameters, without any feature selection process.

LSTM+Logistic: incorporates the important features obtained from the XGBoost and SHAP feature selection process as inputs, and employs a Logistic model to learn and capture the essential feature information. In the time-series information process, all features are included as inputs.

LSTM+MLP: the important features are selected through the XGBoost and SHAP feature selection process, utilizing the MLP output. In the time-series information process, all features are included except for the important features.

LSTM_rnet: the XGBoost and SHAP feature selection process is utilized to select important

features, leveraging the MLP output. Additionally, in the time-series information process, all features are included as inputs.

The experimental results are presented in Table 3. Our LSTMRnet model demonstrates a superior performance on the validation set across five evaluation metrics: MSE, MAE, R² Score, F1 score, and Recall, achieving values of 0.483, 0.373, 0.515, 0.291, and 0.248, respectively. The experimental performance of either the MLP or LSTM is found to be unsatisfactory. The suboptimal performance is attributed to the fact that a single model cannot adequately utilize the feature information, resulting in a poor prediction performance of the respiratory parameters. The LSTM+MLP model incorporates a feature selection step. However, the model separately inputs important and non-important features, leading to an incomplete utilization of the feature set and hampering the connection between features. Overall, the experimental results indicate that our model outperforms the other widely used ML models, which indicates that LSTMRnet can thoroughly learn information from different dimensions of input features. The proposed LSTMRnet model is designed to address the limitations of the other models, and it exhibits superior performance in both regression and classification tasks for ventilator parameter prediction.

Table 3. Comparative experimental results.

Models	Datasets	MSE	MAE	R ² Score	Precision	F1 Score	Recall
MLP	Train	0.557	0.417	0.444	0.374	0.197	0.168
	Val	0.544	0.412	0.453	0.359	0.196	0.171
LSTM	Train	0.496	0.386	0.505	0.420	0.251	0.209
	Val	0.493	0.380	0.508	0.369	0.234	0.203
LSTM+Logistic	Train	0.556	0.416	0.441	0.298	0.171	0.152
	Val	0.551	0.415	0.445	0.299	0.181	0.161
LSTM+MLP	Train	0.524	0.394	0.473	0.378	0.233	0.204
	Val	0.507	0.384	0.491	0.417	0.270	0.232
LSTMRnet	Train	0.477	0.373	0.524	0.571	0.362	0.311
	Val	0.483	0.373	0.515	0.414	0.291	0.248

5. Discussion

5.1. Ablation studies

The effects of different time-series models: We conduct comparative experiments with different sequence models to investigate the effect of the LSTM model on the time-series information process. The XGS-RNN model and XGS-GRU model represent the use of RNN and GRU models, respectively, in the time-series information process. The compared models adopt the top five important features in the important feature information process with the same hyperparameters. The performance of different sequence models on the dataset is shown in Table 4. Our proposed LSTMRnet slightly outperforms the XGS-GRU model, demonstrating the superiority of the proposed method. Both LSTM and GRU can preserve time-series information through gate structures, ensuring that long sequences are maintained during propagation. However, the respiratory dataset has a long sequence, where the longest treatment sequence for patients is 238 steps. The more complex structure of LSTM can capture longer time-series

information, leading to a better performance than GRU.

Table 4. The effects of different time-series models.

Algorithm	Datasets	MSE	MAE	R ² Score	Precision	F1 Score	Recall
XGS-GRU	Train	0.497	0.381	0.497	0.427	0.241	0.204
	Val	0.493	0.382	0.496	0.385	0.236	0.201
XGS-RNN	Train	0.502	0.384	0.494	0.358	0.234	0.201
	Val	0.503	0.380	0.493	0.356	0.236	0.202
LSTMRnet	Train	0.477	0.373	0.524	0.571	0.362	0.311
	Val	0.483	0.373	0.515	0.414	0.291	0.248

The effects of varying LSTM units on the model: Table 5 illustrates the impact of different LSTM unit numbers on the model. As shown in the table, the model with 50 LSTM units outperforms the models with 10 and 30 LSTM units in various indicators of the validation set. Increasing the number of LSTM units in the model enhances its ability to learn historical information, allowing the model to learn more feature time-series information.

Table 5. The effects of different LSTM units.

LSTM units	Datasets	MSE	MAE	R ² Score	Precision	F1 Score	Recall
10	Train	0.536	0.398	0.461	0.316	0.178	0.157
	Val	0.534	0.399	0.463	0.389	0.204	0.176
30	Train	0.506	0.383	0.491	0.364	0.219	0.189
	Val	0.505	0.383	0.493	0.370	0.220	0.191
50	Train	0.477	0.373	0.524	0.571	0.362	0.311
	Val	0.483	0.373	0.515	0.414	0.291	0.248

The effects of a varying number of important features on the model: To study the impact of different numbers of important features on the overall model, we conduct comparative experiments by selecting the top-five, top-ten, and all features based on the feature importance graph. Our goal is to investigate the extent to which the LSTMRnet model's accuracy can be improved with different numbers of important features. Table 6 presents the effects of varying important features on the model. As illustrated in the table, the model using the top five important features achieved the best performance on the validation set, with an MSE of 0.483 and a Precision of 0.414. This indicates that the top-five important features have the greatest impact on the output, which is consistent with the results of the SHAP analysis, as the SHAP values of the top five important features are higher than the average. Increasing the number of important features resulted in a decrease in prediction performance, which might be mainly due to the increased number of less important features, making it difficult for the model to accurately learn the relationship between input and output.

Table 6. The effects of different important feature numbers.

Feature numbers	Datasets	MSE	MAE	R ² Score	Precision	F1 Score	Recall
5	Train	0.477	0.373	0.524	0.571	0.362	0.311
	Val	0.483	0.373	0.515	0.414	0.291	0.248
10	Train	0.494	0.381	0.503	0.405	0.233	0.198
	Val	0.498	0.382	0.498	0.392	0.250	0.213
14	Train	0.494	0.381	0.502	0.419	0.265	0.223
	Val	0.490	0.380	0.506	0.385	0.258	0.221

The effects of different concatenate strategies on the model: Additionally, we explore the effects of different fusion methods of the important feature selection and time-series information capture processes. The first strategy is concatenation (Concat), which is commonly used to combine features by merging different dimensions of output layer information, thereby increasing the vector's dimensions. The second strategy is addition (Add), which adds the output of two-dimensional feature information without increasing the vector's dimensions. According to Table 7, the Concat strategy is superior to the addition strategy. The principal idea of LSTMRnet is to primarily use a time-series model to improve the predictive performance of the model by strengthening the expression of important features. The Add strategy will directly superimpose the time-series information and important feature information, increasing the amount of information that describes the patient's condition, but only slightly improving the overall performance of the model. Both blood gas analysis indicators and vital sign monitoring data have time-series features, but blood gas analysis indicators have greater clinical reference values. Thus, the fusion method of Concat in our LSTMRnet model will enhance the expression of different types of features, which also better conforms to the rules of ventilator parameter settings.

Table 7. The effects of different concatenate strategies.

Fusion Method	Datasets	MSE	MAE	R ² Score	Precision	F1 Score	Recall
Concat	Train	0.477	0.373	0.524	0.571	0.362	0.311
	Val	0.483	0.373	0.515	0.414	0.291	0.248
Add	Train	0.499	0.382	0.498	0.276	0.186	0.164
	Val	0.502	0.384	0.495	0.338	0.214	0.192

5.2. Clinical relevance

Our study is significant to clinical usage because the precise prediction of patient-specific ventilator parameters is crucial for optimizing patient-ventilator interaction and selecting appropriate treatment interventions. Inaccurate prediction can lead to ineffective or harmful treatments, potentially compromising patient safety and care. The proposed LSTMRnet model overcomes these limitations by simultaneously obtaining essential time-series and feature information, and identifying crucial factors affecting respiratory parameters. Our study has the potential to improve clinical outcomes and patient care, particularly in the context of sleep apnea-hypopnea syndrome and ventilator treatment in ICUs. The validation of the proposed model on a large dataset demonstrates its

superiority over competing models, indicating its potential use in clinical practice. As a result, our model has significant clinical implications and has the potential to improve patient outcomes and quality of care.

6. Conclusions

We present a novel long short-term memory relation network (i.e., LSTMRnet) for ventilator parameter prediction. We tackle both continuous and discrete ventilator parameter prediction based on the large medical dataset MIMIC-III. Our model benefits from both spatial and time-series information while maintaining both features to produce predictions with a higher degree of accuracy. We extensively validate its superiority by comparing it with conventional ML techniques in public benchmark datasets, and our model demonstrates the superiority over other state-of-the-art methods. In the future, we will validate it through more *in-vitro* and *in-vivo* experiments to make it more applicable in clinical usages.

Use of AI tools declaration

The authors declare they have not used Artificial Intelligence (AI) tools in the creation of this article.

Acknowledgments

This work is supported by the National Natural Science Foundation of China, “Science and Technology Innovation Action Plan” Shanghai Natural Science Foundation, Shanghai Municipal Key Clinical Specialty, China (Grant No.62102241, No.23ZR1425400, No.shslczdzk00801).

References

1. P. H. Wicky, M. S. Niedermann, J. F. Timsit, Ventilator-associated pneumonia in the era of COVID-19 pandemic: How common and what is the impact?, *Crit. Care*, **25** (2021), 1–3. <https://doi.org/10.1186/s13054-021-03571-z>
2. M. M. Cvach, J. E. Stokes, S. H. Manzoor, P. O. Brooks, T. S. Burger, A. Gottschalk, et al., Ventilator alarms in intensive care units: frequency, duration, priority, and relationship to ventilator parameters, *Anesth. Analg.*, **130** (2020), 9–13. <https://doi.org/10.1213/ANE.0000000000003801>
3. S. C. Auld, M. Caridi-Scheible, J. M. Blum, C. Robichaux, C. Kraft, J. T. Jacob, et al., ICU and ventilator mortality among critically ill adults with coronavirus disease 2019, *Crit. Care Med.*, **48** (2020), 799–804. <https://doi.org/10.1097/CCM.0000000000004457>
4. N. J. Meyer, L. Gattinoni, C. S. Calfee, Acute respiratory distress syndrome, *Lancet*, **398** (2021), 622–637. [https://doi.org/10.1016/S0140-6736\(21\)00439-6](https://doi.org/10.1016/S0140-6736(21)00439-6)
5. R. Chand, E. R. Swenson, D. S. Goldfarb, Sodium bicarbonate therapy for acute respiratory acidosis, *Curr. Opin. Nephrol. Hypertens.*, **30** (2021), 223–230. <https://doi.org/10.1097/MNH.0000000000000687>

6. T. Nemoto, G. E. Hatzakis, C. W. Thorpe, R. Olivenstein, S. Dial, J. H. T. Bates, Automatic control of pressure support mechanical ventilation using fuzzy logic, *Am. J. Respir. Crit. Care Med.*, **160** (1999), 550–556. <https://doi.org/10.1164/ajrccm.160.2.9809013>
7. S. E. Rees, C. Allerød, D. Murley, Y. Zhao, B. W. Smith, S. Kjaergaard, et al., Using physiological models and decision theory for selecting appropriate ventilator settings, *J. Clin. Monit. Comput.*, **20** (2006), 421–429. <https://doi.org/10.1007/s10877-006-9049-5>
8. D. S. Karbing, C. Allerød, L. P. Thomsen, K. Espersen, P. Thorgaard, S. Andreassen, et al., Retrospective evaluation of a decision support system for controlled mechanical ventilation, *Med. Biol. Eng. Comput.*, **50** (2012), 43–51. <https://doi.org/10.1007/s11517-011-0843-y>
9. R. L. Chatburn, E. Mireles-Cabodevila, Closed-loop control of mechanical ventilation: description and classification of targeting schemes, *Respir. Care*, **56** (2011), 85–102. <https://doi.org/10.4187/respcare.00967>
10. F. D. Marco, S. Centanni, A. Bellone, G. Messinesi, A. Pesci, R. Scala, et al., Optimization of ventilator setting by flow and pressure waveforms analysis during noninvasive ventilation for acute exacerbations of COPD: a multicentric randomized controlled trial, *Crit. Care*, **15** (2011), 1–9. <https://doi.org/10.1186/cc10567>
11. D. S. Karbing, S. Spadaro, N. Dey, R. Ragazzi, E. Marangoni, F. D. Corte, et al., An open-loop, physiologic model-based decision support system can provide appropriate ventilator settings, *Crit. Care Med.*, **46** (2018), 642–648. <https://doi.org/10.1097/CCM.00000000000003133>
12. N. Burkart, N. F. Huber, A survey on the explainability of supervised machine learning, *J. Artif. Intell. Res.*, **70** (2021), 245–317. <https://doi.org/10.1613/jair.1.12228>
13. S. Kushwaha, S. Bahl, A. K. Bagha, K. S. Parmar, M. Javaid, A. Haleem, et al., Significant applications of machine learning for COVID-19 pandemic, *J. Ind. Integr. Manage.*, **5** (2020), 453–479. <https://doi.org/10.1142/S2424862220500268>
14. Y. Ru, X. Qiu, X. Tan, B. Chen, Y. Gao, Y. Jin, Sparse-attentive meta temporal point process for clinical decision support, *Neurocomputing*, **485** (2022), 114–123. <https://doi.org/10.1016/j.neucom.2022.02.028>
15. A. S. Kwekha-Rashid, H. N. Abduljabbar, B. Alhayani, Coronavirus disease (COVID-19) cases analysis using machine-learning applications, *Appl. Nanosci.*, **13** (2023), 2013–2025. <https://doi.org/10.1007/s13204-021-01868-7>
16. L. Yang, A. Shami, On hyperparameter optimization of machine learning algorithms: Theory and practice, *Neurocomputing*, **415** (2020), 295–316. <https://doi.org/10.1016/j.neucom.2020.07.061>
17. X. Qiu, X. Tan, Q. Li, S. Chen, Y. Ru, Y. Jin, A latent batch-constrained deep reinforcement learning approach for precision dosing clinical decision support, *Knowl.-Based Syst.*, **237** (2022), 107689. <https://doi.org/10.1016/j.knosys.2021.107689>
18. M. Barish, S. Bolourani, L. F. Lau, S. Shah, T. P. Zanos, External validation demonstrates limited clinical utility of the interpretable mortality prediction model for patients with COVID-19, *Nat. Mach. Intell.*, **3** (2021), 25–27. <https://doi.org/10.1038/s42256-020-00254-2>

19. X. Li, H. Xiong, X. Li, X. Wu, X. Zhang, J. Liu, et al., Interpretable deep learning: Interpretation, interpretability, trustworthiness, and beyond, *Knowl. Inf. Syst.*, **64** (2022), 3197–3234. <https://doi.org/10.1007/s10115-022-01756-8>
20. S. Chen, X. Qiu, X. Tan, Z. Fang, Y. Jin, A model-based hybrid soft actor-critic deep reinforcement learning algorithm for optimal ventilator settings, *Inf. Sci.*, **611** (2022), 47–64. <https://doi.org/10.1016/j.ins.2022.08.028>
21. H. Carmichael, J. Coquet, R. Sun, S. Sang, D. Groat, S. M. Asch, et al., Learning from past respiratory failure patients to triage COVID-19 patient ventilator needs: A multi-institutional study, *J. Biomed. Inf.*, **119** (2021), 103802. <https://doi.org/10.1016/j.jbi.2021.103802>
22. F. P. Akbulut, E. Akkur, A. Akan, B. S. Yarman, A decision support system to determine optimal ventilator settings, *BMC Med. Inf. Decis. Making*, **14** (2014), 1–11. <https://doi.org/10.1186/1472-6947-14-3>
23. S. Ghazal, M. Sauthier, D. Brossier, W. Bouachir, P. A. Jouvet, R. Noumeir, Using machine learning models to predict oxygen saturation following ventilator support adjustment in critically ill children: A single center pilot study, *PloS One*, **14** (2019), 0198921. <https://doi.org/10.1371/journal.pone.0198921>
24. A. Peine, A. Hallawa, J. Bickenbach, G. Dartmann, L. B. Fazlic, A. Schmeink, et al., Development and validation of a reinforcement learning algorithm to dynamically optimize mechanical ventilation in critical care, *NPJ. Digit. Med.*, **4** (2021), 32. <https://doi.org/10.1038/s41746-021-00388-6>
25. S. Radhakrishnan, S. G. Nair, J. Isaac, Multilayer perceptron neural network model development for mechanical ventilator parameters prediction by real time system learning, *Biomed. Signal Process. Control*, **71** (2022), 103170. <https://doi.org/10.1007/s10877-006-9049-5>
26. M. A. Deif, A. A. A. Solyman, M. H. Alsharif, P. Uthansakul, Automated triage system for intensive care admissions during the COVID-19 pandemic using hybrid XGBoost-AHP approach, *Sensors*, **21** (2021), 6379. <https://doi.org/10.3390/s21196379>
27. L. Zhuo, M. Yoneda, M. Zhao, W. Yingsung, N. Yoshida, Y. Kitagawa, et al., Defect in SHAP-hyaluronan complex causes severe female infertility: A study by inactivation of the bikunin gene in mice, *J. Biol. Chem.*, **276** (2001), 7693–7696. <https://doi.org/10.1074/jbc.C000899200>
28. H. Niu, K. Xu, A hybrid model combining variational mode decomposition and an attention-GRU network for stock price index forecasting, *Math. Biosci. Eng.*, **17** (2020), 7151–7166. <https://doi.org/10.3934/mbe.2020367>
29. F. Tehrani, M. Rogers, T. Lo, T. Malinowski, S. Afuwape, M. Lum, et al., A dual closed-loop control system for mechanical ventilation, *J. Clin. Monit. Comput.*, **18** (2004), 111–129. <https://doi.org/10.1023/B:JOCM.0000032744.99885.38>
30. L. Yan, H. T. Zhang, J. Goncalves, X. Yang, M. Wang, Y. Guo, et al., An interpretable mortality prediction model for COVID-19 patients, *Nat. Mach. Intell.*, **2** (2020), 283–288. <https://doi.org/10.1038/s42256-020-0180-7>
31. W. Chen, H. Huang, P. Ko, W. Su, C. Kao, S. Su, A simple algorithm using ventilator parameters to predict successfully rapid weaning program in cardiac intensive care unit patients, *J. Pers. Med.*, **12** (2022), 501. <https://doi.org/10.3390/jpm12030501>

32. Y. Zhu, J. Zhang, G. Wang, R. Yao, C. Ren, C. Chen, et al., Machine learning prediction models for mechanically ventilated patients: analyses of the MIMIC-III database, *Front. Med.*, **8** (2021), 955. <https://doi.org/10.3389/fmed.2021.662340>
33. S. S. O. Venkata, A. Koenig, R. M. Pidaparti, Mechanical ventilator parameter estimation for lung health through machine learning, *Bioengineering*, **8** (2021), 60. <https://doi.org/10.3390/bioengineering8050060>
34. A. I. A. Osman, A. N. Ahmed, M. F. Chow, Y. F. Huang, A. El-Shafie, Extreme gradient boosting (Xgboost) model to predict the groundwater levels in Selangor Malaysia, *Ain Shams Eng. J.*, **12** (2021), 1545–1556. <https://doi.org/10.1016/j.asej.2020.11.011>
35. K. Aas, M. Jullum, A. Løland, Explaining individual predictions when features are dependent: More accurate approximations to Shapley values, *Artif. Intell.*, **298** (2021), 103502. <https://doi.org/10.1016/j.artint.2021.103502>
36. A. Chaddad, J. Peng, J. Xu, A. Bouridane, Survey of explainable AI techniques in healthcare, *Sensors*, **23** (2023), 634. <https://doi.org/10.3390/s23020634>
37. Y. Meng, N. Yang, Z. Qian, G. Zhang, What makes an online review more helpful: An interpretation framework using XGBoost and SHAP values, *J. Theor. Appl. Electron. Commer. Res.*, **16** (2021), 466–490. <https://doi.org/10.3390/jtaer16030029>
38. G. Van Houdt, C. Mosquera, G. Nápoles, A review on the long short-term memory model, *Artif. Intell. Rev.*, **53** (2020), 5929–5955. <https://doi.org/10.1007/s10462-020-09838-1>
39. Z. He, Y. Gao, X. Wang, Analysis of related factors of 48 non-survivors transferred or re-admitted to intensive care unit, *Chin. Crit. Care Med.*, **18** (2006), 740–742.
40. L. Zhao, J. Liu, J. Ren, Impact of various ventilation modes on IAQ and energy consumption in Chinese dwellings: First long-term monitoring study in Tianjin, China, *Buil. Environ.*, **143** (2018), 99–106. <https://doi.org/10.1016/j.buildenv.2018.06.057>
41. S. Cao, C. Ren, Ventilation control strategy using low-dimensional linear ventilation models and artificial neural network, *Buil. Environ.*, **144** (2018), 316–333. <https://doi.org/10.1016/j.buildenv.2018.08.032>
42. G. Bellani, A. Grassi, S. Sosio, S. Gatti, B. P. Kavanagh, A. Pesenti, et al., Driving pressure is associated with outcome during assisted ventilation in acute respiratory distress syndrome, *Anesthesiology*, **131** (2019), 594–604. <https://doi.org/10.1097/ALN.0000000000002846>



AIMS Press

©2023 the Author(s), licensee AIMS Press. This is an open access article distributed under the terms of the Creative Commons Attribution License (<http://creativecommons.org/licenses/by/4.0>)